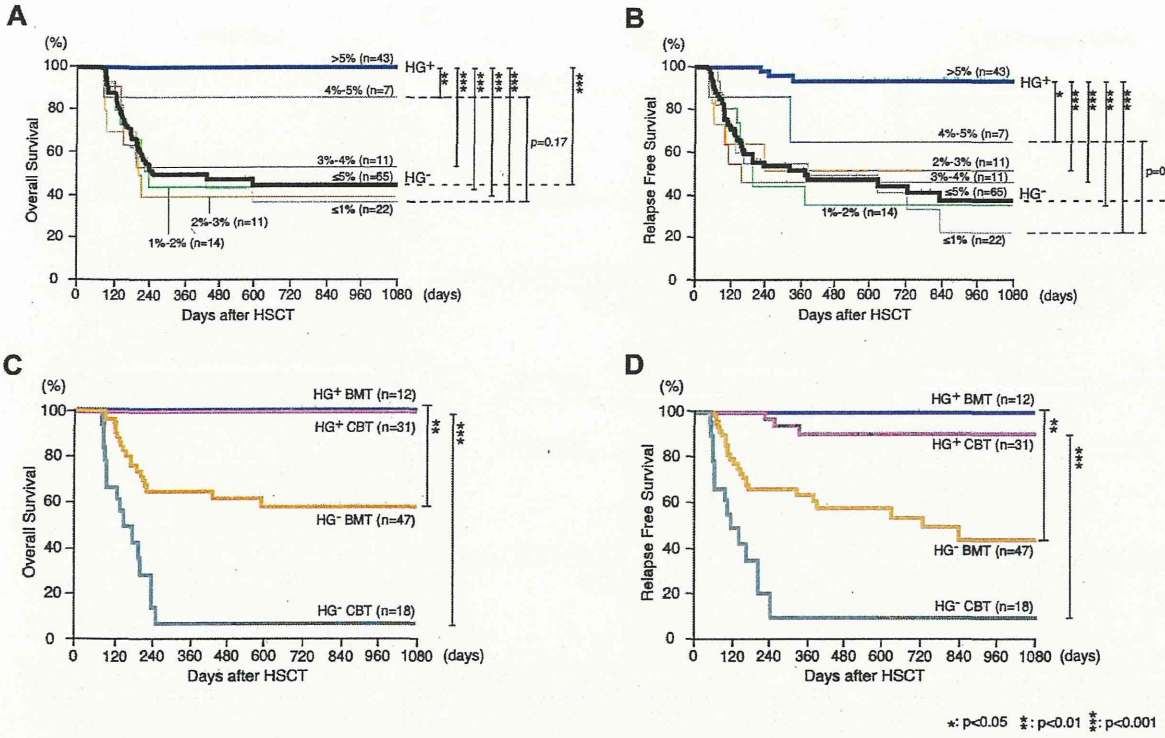

Figure 3. Patients whose hematogones comprised > 5% bone marrow MNCs constitute a group with significantly improved survival, irrespective of HSC sources. (A-B) The Kaplan-Meier estimates of (A) OS and (B) RFS among patient subgroups with ≤ 1% (gray line), 1%-2% (green line), 2%-3% (orange line), 3%-4% (red line), 4%-5% (purple line), ≤ 5% (black bold line), or > 5% (blue bold line) hematogones in the bone marrow MNCs. Forty-three patients who developed > 5% MNC hematogones (HG^+) showed significantly better 3-year OS and RFS, compared with any of each group ($P < .01$ and $P < .05$, respectively), as well as to 65 patients with ≤ 5% MNCs hematogones (HG^-; $P < .001$ for both). (C-D) The Kaplan-Meier estimates of (C) OS and (D) RFS in HG^+ and HG^- groups that received transplants with BMT or CBT. The improved OS and RFS were seen in HG^+ groups regardless of the source of HSC. HG^+ indicates patients developed hematogones (> 5% of bone marrow MNCs); HG^- indicates patients who failed to develop hematogones (≤ 5% of bone marrow MNCs).

acute GVHD (2 patients) and viral infections (4 patients). Of the 26 patients who died of primary disease, 24 developed both acute GVHD and infections.

We analyzed the relationship between the emergence of documented hematogones in the bone marrow, and variables including sex of donor/recipient, days required for engraftment, primary diseases, times of intensive chemotherapy before HSCT, remission status, conditioning regimen, documented infectious disease, and episode of acute/chronic GVHD by using univariate and multivariate analysis. These analyses were performed in patient groups treated with BMT and CBT, respectively.

There were no correlations found between the emergence of > 5% of hematogones and clinical factors such as the day of engraftment, primary disease, times of intensive chemotherapies, and remission status, in either univariate or multivariate analyses. As shown in Table 4, in univariate analysis, a hematogone increase up to > 5% of MNCs was found more frequently in patients without viral infection (such as cytomegalovirus, human herpesvirus 6, and adenovirus; BMT: $P = .03$; CBT: $P < .01$), and those did not develop severe acute GVHD of grade II-IV (BMT: $P < .01$; CBT: $P < .01$). Time required for engraftment did not differ between patient groups with or without infections, or acute GVHD (Table 2). These data appear to be compatible with the analysis of causes of death in HG^- patients (Table 3). On the other hand, in multivariate analysis, severe acute GVHD of grade II-IV, but not infection was the significant risk factor for emergence of hematogones (BMT: $P = .03$; CBT: $P = .04$; Table 4). Based on these analyses, the emergence of hematogones heralds less frequent development of severe acute GVHD.

Discussion

Hematogones are immature B-cell precursors that reside mainly in the bone marrow of every normal individual,[1,2,27,40] and their numbers could reflect activity of normal B lymphopoiesis. Hematogones are occasionally seen in large numbers in healthy people, especially in infants and young children.[2,4,7,8] Interestingly, recent reports have suggested that the presence of detectable numbers of hematogones at the recovery phase from myelosuppression reflects better prognosis of patients with AML treated with chemotherapy[5] or CBT,[6] although the underlying mechanism of this phenomenon is unclear. The increase of hematogones may reflect eradication of leukemic cells that could inhibit normal hematopoiesis,[1,5] or rapid immune reconstitution that could suppress infection and severe acute GVHD in an allogeneic HSCT setting.[6]

In these reports, the presence of hematogones was documented when they were detectable at a low frequency: ≥ 0.01% of TNCs at a recovery phase[5] or > 0% and > 0.9% of MNCs on day 21 and 100, respectively.[6] In contrast, the patient cohort in our study received allogeneic HSCT, and the majority (106 of 108 cases) of patients had > 0.1% of hematogones at engraftment by our multicolor flow cytometric analysis (Figure 1C). Therefore, it was critical to set an appropriate threshold value and timing of sampling

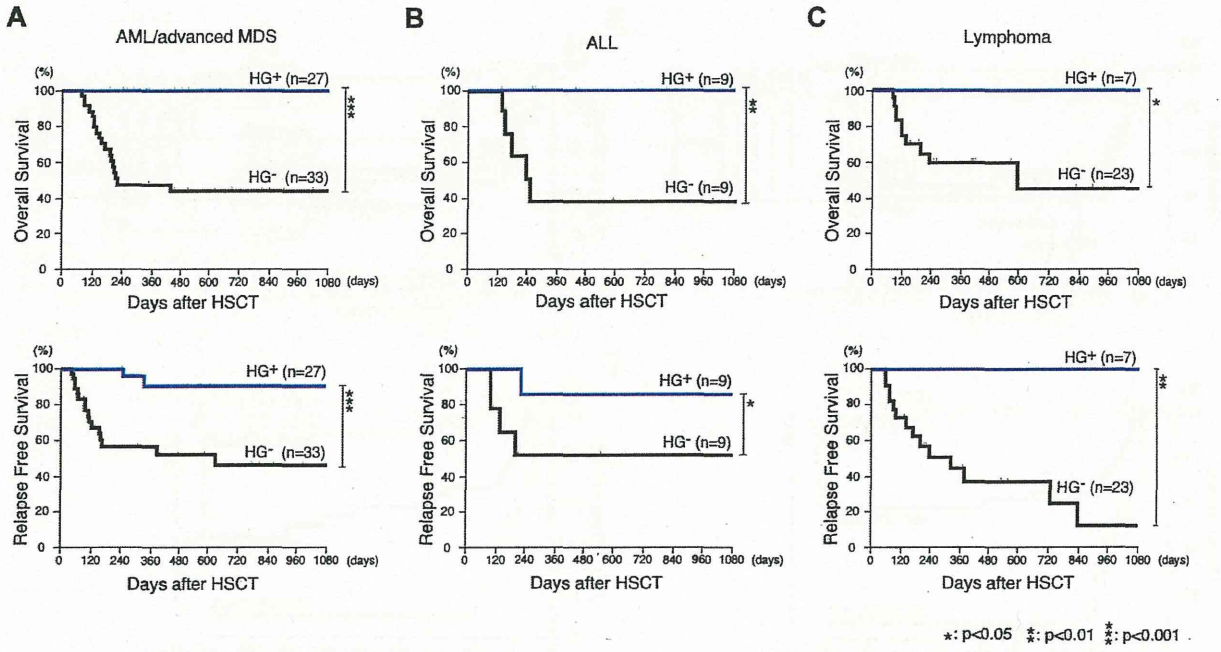

Figure 4. Patients who developed > 5% hematogones as a fraction of their MNCs constitute a group with significantly improved survival, irrespective of their primary disease. The Kaplan-Meier estimates of OS and RFS in HG$^+$ and HG$^-$ patients differentiated with their primary disease. In each group of patients with (A) AML or advanced MDS, (B) ALL, and (C) lymphoma, HG$^+$ groups showed significantly better OS and RFS, compared with the HG$^-$ group ($P < .001$ for both).

to decide a clinically meaningful increase of hematogones in an allogeneic HSCT setting. Furthermore, previous studies were performed only in patients with AML,[5,6] but not in patients with lymphoid neoplasms, presumably because it was difficult to discriminate a small number of neoplastic lymphoid cells from hematogones.[6]

To accurately enumerate hematogones in patients with various clinical backgrounds and with different donor cell sources, we performed the analysis on the day when patients met the clinical criteria of engraftment[9-12] and displayed complete donor-type chimerism. The confirmation for donor-type chimerism allowed us to avoid miscounting neoplastic lymphoid cells as hematogones. Because these samples should be free from host-derived cells, we included patients with lymphoid malignancies in our study. We rigorously measured the frequencies of hematogones within bone marrow MNCs by 6-color flow cytometric analysis.

In our study, donor-derived hematogones were polyclonal, based on *IGH* rearrangement analysis in all cases, and therefore the presence of hematogones should be a snapshot of normal B lymphopoiesis at the recovery phase. In fact, the frequencies of hematogones at engraftment were correlated with circulating B-cell numbers at least until day 90 (Figure 2). Importantly, we here show that the frequencies of hematogones were correlated with donors' age, but not with recipients' age, suggesting the age-dependent decline of B-cell potential of donor HSCs. This is compatible with previous mouse studies in which younger HSCs are capable of producing more abundant B cells.[41-43]

According to our criteria, the engraftment was seen on days 25 and 32 (median) in BMT and CBT groups (Figure 1D), respectively, consistent with previous studies.[35-39,44] Within each BMT or CBT group, the engraftment day was not significantly altered by the patients' primary disease or remission status at transplantation (Table 2). The bone marrow sampling for hematogone analysis was performed on the day of engraftment. As shown in Table 3, the timing of sampling (= the day of engraftment) was not significantly related to emergence of hematogones in univariate and multivariate analyses. Interestingly, however, our data suggest that when hematogones reach > 5% of MNCs at engraftment, it has a profound clinical impact on patients' OS and RFS (Figure 3A-B). It is of note that the emergence of documented hematogones

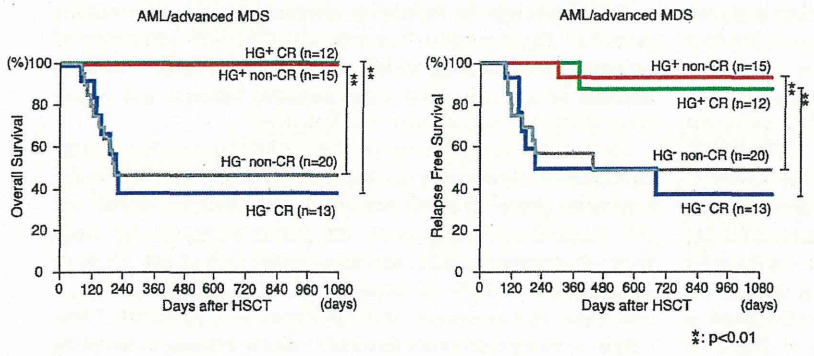

Figure 5. The presence of hematogones marks a group with good prognosis in AML/advanced MDS patients. The Kaplan-Meier estimates of OS and RFS in HG$^+$ and HG$^-$ patients in AML or advanced MDS differentiated with their remission status before HSCT. Significantly better OS and RFS were seen in HG$^+$ groups irrespective of their remission status.

Table 3. Cause of death in patients with less than 5% hematogones

	Cause of death, no. (%)					
	Relapse of primary disease			Transplantation-related mortality		
Primary disease	Infection	Acute GVHD (Grade II-IV)	Total	Infection	Acute GVHD (Grade II-IV)	Total
AML and advanced MDS	14/33 (42.4)	14/33 (42.4)	15/33 (45.4)	2/33 (6.1)	0/33 (0)	2/33 (6.1)
ALL	3/9 (33.3)	3/9 (33.3)	3/9 (33.3)	1/9 (11.1)	1/9 (11.1)	2/9 (22.2)
Lymphoma	7/23 (30.4)	7/23 (30.4)	8/23 (34.8)	1/23 (4.3)	1/23 (4.3)	2/23 (8.7)
Total	24/65 (36.9)	24/65 (36.9)	26/65 (40)	4/65 (6.2)	2/65 (3.1)	6/65 (9.2)

ALL indicates acute lymphoblastic leukemia; AML, acute myelogenous leukemia; GVHD, graft-versus-host disease; and MDS, myelodysplastic syndrome.

was not related to times of intensive chemotherapies or remission status of patients before transplantation in both univariate and multivariate analyses (Table 3). This result suggests that the emergence of hematogones was not affected by the potential damage of host microenvironment through multiple chemotherapies.

The improvement of OS and RFS in HG^+ patients was seen in all patient groups: those suffering from AML/advanced MDS, ALL, or lymphoma (Figure 4). Furthermore, this effect became more evident when patients who had failed to achieve CR before transplantation were analyzed (Figure 5). In this case, the appearance of hematogones clearly marks a subgroup with favorable OS and RFS, irrespective of their primary diseases. In contrast, in patients who had achieved CR before transplantation, prolonged OS and RFS were found only in patients with AML/advanced MDS, but not in patients with ALL or lymphoma (Figure 5). A larger study including higher number of patients should be performed to clarify the impact of hematogones on HSCT results in CR patients with lymphoid malignancies.

The analyses of risk factors for the appearance of > 5% MNCs of hematogones revealed that in both BMT and CBT patients, the less frequent occurrences of severe acute GVHD and infections were significantly correlated in univariate analyses, whereas the less frequent severe acute GVHD was the only risk factor in multivariate analyses (Table 3). As shown in Table 4, all 32 deaths occurred only in HG^- patients, and 24 of these 32 patients developed both severe acute GVHD and infection before the relapse of the disease. In these patients, doses of immunosuppressive drugs were escalated to control acute GVHD, which might cause development of infections as well as recurrence of primary disease.[6,45,46] It is therefore possible that less frequent development of severe acute GVHD in HG^+ patients is one of the reasons for their better OS and RFS.

The rapid reconstitution of the immune system represented by a high number of hematogones should be able to prevent infection.[6,45] In turn, successful prevention of acute GVHD could result in proliferation of hematogones because acute GVHD itself may suppress hematopoietic recovery by targeting the bone marrow HSC niche[47] or by attacking directly B-lymphoid cells.[46] In addition, the fact that improvement of RFS is associated with the expansion of hematogones suggests an interesting possibility that B cells play a role in the graft-versus-leukemia effect,[48] although this is still controversial.[41] Also in turn, it is possible that the successful eradication of neoplastic cells from the bone marrow by HSCT results simply in rapid expansion of hematogones.

Thus, our data suggest that the expansion of hematogones is a useful indicator to discriminate a patient group with improved OS and RFS after allogeneic HSCT. Based on rigorous evaluation of frequencies of hematogones after HSCT, we propose that 5% of MNCs is a threshold value for a clinically valuable increase of hematogones. The prognostic value of this definition should be tested by future studies in larger groups of patients.

Acknowledgments

The authors thank the medical and nursing staff working on the Fukuoka Blood and Marrow Transplantation Group for providing patient information, and D. Dalma-Weiszhausz for critically reviewing the manuscript.

This work was supported, in part, by a Grant-in-Aid from the Ministry of Education, Culture, Sports, Science, and Technology of Japan (K.A., T.M.).

Authorship

Contribution: T.S. and T.M. coordinated the project, designed and performed the transplantation and experiments, analyzed the data, and wrote the manuscript; Y.K., Y.M., K. Kamezaki, K. Takenaka, H.I., K.N., T.T, and K. Kato performed the transplantation and provided technical advice; K. Takase, H.H., A.N., Y.I., T.K., and T.E. provided patient information, clinical samples, and technical advice; and K.A. designed the experiments, reviewed the data, and edited the manuscript.

Conflict-of-interest disclosure: The authors declare no competing financial interests.

Correspondence: Koichi Akashi, Department of Medicine and Biosystemic Sciences, Kyushu University Graduate School of Medicine, 3-1-1 Maidashi, Higashi-ku, Fukuoka 812-0054, Japan; e-mail: akashi@med.kyushu-u.ac.jp.

Table 4. Risk factors for development of more than 5% MNCs of hematogone based on univariate and multivariate analyses

	BMT				CBT			
	Univariate		Multivariate		Univariate		Multivariate	
	Odds ratio (95% CI)	*P*	Odds ratio (95% CI)	*P*	Odds ratio (95% CI)	*P*	Odds ratio (95% CI)	*P*
Infections, Yes/No	0.19 (0.05-0.74)	.03	0.42 (0.02-1.58)	.23	0.16 (0.04-0.57)	< .01	0.37 (0.02-2.81)	.10
Acute GVHD, Grade II-IV/0-I	0.09 (0.01-0.73)	< .01	0.04 (0.00-0.85)	.03	0.12 (0.03-0.48)	< .01	0.04 (0.00-0.80)	.04

BMT indicates bone marrow transplantation; CBT, cord blood transplantation; CI, confidence interval; GVHD, graft-versus-host disease; and MNC, mononuclear cell.

References

1. McKenna RW, Washington LT, Aquino DB, Picker LJ, Kroft SH. Immunophenotypic analysis of hematogones (B-lymphocyte precursors) in 662 consecutive bone marrow specimens by 4-color flow cytometry. *Blood.* 2001;98(8):2498-2507.
2. Sevilla DW, Colovai AI, Emmons FN, Bhagat G, Alobeid B. Hematogones: a review and update. *Leuk Lymphoma.* 2010;51(1):10-19.
3. Muehleck SD, McKenna RW, Gale PF, Brunning RD. Terminal deoxynucleotidyl transferase (TdT)-positive cells in bone marrow in the absence of hematologic malignancy. *Am J Clin Pathol.* 1983;79(3):277-284.
4. Davis RE, Longacre TA, Cornbleet PJ. Hematogones in the bone marrow of adults. Immunophenotypic features, clinical settings, and differential diagnosis. *Am J Clin Pathol.* 1994;102(2):202-211.
5. Chantepie SP, Salaun V, Parienti JJ, et al. Hematogones: a new prognostic factor for acute myeloblastic leukemia. *Blood.* 2011;117(4):1315-1318.
6. Honebrink T, Dayton V, Burke MJ, et al. Impact of bone marrow hematogones on umbilical cord blood transplantation outcomes in patients with acute myeloid leukemia. *Biol Blood Marrow Transplant.* 2012;18(6):930-936.
7. Brady KA, Atwater SK, Lowell CA. Flow cytometric detection of CD10 (cALLA) on peripheral blood B lymphocytes of neonates. *Br J Haematol.* 1999;107(4):712-715.
8. Longacre TA, Foucar K, Crago S, et al. Hematogones: a multiparameter analysis of bone marrow precursor cells. *Blood.* 1989;73(2):543-552.
9. Dreger P, Kloss M, Petersen B, et al. Autologous progenitor cell transplantation: prior exposure to stem cell-toxic drugs determines yield and engraftment of peripheral blood progenitor cell but not of bone marrow grafts. *Blood.* 1995;86(10):3970-3978.
10. Davies SM, Kollman C, Anasetti C, et al. Engraftment and survival after unrelated-donor bone marrow transplantation: a report from the national marrow donor program. *Blood.* 2000;96(13):4096-4102.
11. Bensinger WI, Martin PJ, Storer B, et al. Transplantation of bone marrow as compared with peripheral-blood cells from HLA-identical relatives in patients with hematologic cancers. *N Engl J Med.* 2001;344(3):175-181.
12. Laughlin MJ, Barker J, Bambach B, et al. Hematopoietic engraftment and survival in adult recipients of umbilical-cord blood from unrelated donors. *N Engl J Med.* 2001;344(24):1815-1822.
13. Dohner H, Estey EH, Amadori S, et al. Diagnosis and management of acute myeloid leukemia in adults: recommendations from an international expert panel, on behalf of the European LeukemiaNet. *Blood.* 2010;115(3):453-474.
14. Greenberg P, Cox C, LeBeau MM, et al. International scoring system for evaluating prognosis in myelodysplastic syndromes. *Blood.* 1997;89(6):2079-2088.
15. Appelbaum FR, Anderson J. Allogeneic bone marrow transplantation for myelodysplastic syndrome: outcomes analysis according to IPSS score. *Leukemia.* 1998;12(Suppl 1):S25-S29.
16. Goldman JM, Schmitz N, Niethammer D, Gratwohl A. Allogeneic and autologous transplantation for haematological diseases, solid tumours and immune disorders: current practice in Europe in 1998. Accreditation Sub-Committee of the European Group for Blood and Marrow Transplantation. *Bone Marrow Transplant.* 1998;21(1):1-7.
17. Perea G, Lasa A, Aventin A, et al. Prognostic value of minimal residual disease (MRD) in acute myeloid leukemia (AML) with favorable cytogenetics [t(8;21) and inv(16)]. *Leukemia.* 2006;20(1):87-94.
18. Cheson BD, Pfistner B, Juweid ME, et al. Revised response criteria for malignant lymphoma. *J Clin Oncol.* 2007;25(5):579-586.
19. Uchida N, Wake A, Takagi S, et al. Umbilical cord blood transplantation after reduced-intensity conditioning for elderly patients with hematologic diseases. *Biol Blood Marrow Transplant.* 2008;14(5):583-590.
20. Kim SW, Matsuo K, Fukuda T, et al. Reduced-intensity unrelated donor bone marrow transplantation for hematologic malignancies. *Int J Hematol.* 2008;88(3):324-330.
21. Oda S, Oki E, Maehara Y, Sugimachi K. Precise assessment of microsatellite instability using high resolution fluorescent microsatellite analysis. *Nucleic Acids Res.* 1997;25(17):3415-3420.
22. Kikushige Y, Yoshimoto G, Miyamoto T, et al. Human Flt3 is expressed at the hematopoietic stem cell and the granulocyte/macrophage progenitor stages to maintain cell survival. *J Immunol.* 2008;180(11):7358-7367.
23. Mori Y, Iwasaki H, Kohno K, et al. Identification of the human eosinophil lineage-committed progenitor: revision of phenotypic definition of the human common myeloid progenitor. *J Exp Med.* 2009;206(1):183-193.
24. Imamura R, Miyamoto T, Yoshimoto G, et al. Mobilization of human lymphoid progenitors after treatment with granulocyte colony-stimulating factor. *J Immunol.* 2005;175(4):2647-2654.
25. Yoshimoto G, Miyamoto T, Jabbarzadeh-Tabrizi S, et al. FLT3-ITD up-regulates MCL-1 to promote survival of stem cells in acute myeloid leukemia via FLT3-ITD-specific STAT5 activation. *Blood.* 2009;114(24):5034-5043.
26. Galy A, Travis M, Cen D, Chen B. Human T, B, natural killer, and dendritic cells arise from a common bone marrow progenitor cell subset. *Immunity.* 1995;3(4):459-473.
27. LeBien TW. Fates of human B-cell precursors. *Blood.* 2000;96(1):9-23.
28. LeBien TW, Tedder TF. B lymphocytes: how they develop and function. *Blood.* 2008;112(5):1570-1580.
29. Yoshimoto G, Nagafuji K, Miyamoto T, et al. FLT3 mutations in normal karyotype acute myeloid leukemia in first complete remission treated with autologous peripheral blood stem cell transplantation. *Bone Marrow Transplant.* 2005;36(11):977-983.
30. Kikushige Y, Ishikawa F, Miyamoto T, et al. Self-renewing hematopoietic stem cell is the primary target in pathogenesis of human chronic lymphocytic leukemia. *Cancer Cell.* 2011;20(2):246-259.
31. Maldonado G, Greenland S. Simulation study of confounder-selection strategies. *Am J Epidemiol.* 1993;138(11):923-936.
32. Baron F, Sandmaier BM. Chimerism and outcomes after allogeneic hematopoietic cell transplantation following nonmyeloablative conditioning. *Leukemia.* 2006;20(10):1690-1700.
33. Matsuda K, Yamauchi K, Tozuka M, et al. Monitoring of hematopoietic chimerism by short tandem repeats, and the effect of CD selection on its sensitivity. *Clin Chem.* 2004;50(12):2411-2414.
34. Boeck S, Hamann M, Pihusch V, et al. Kinetics of dendritic cell chimerism and T cell chimerism in allogeneic hematopoietic stem cell recipients. *Bone Marrow Transplant.* 2006;37(1):57-64.
35. Laughlin MJ, Eapen M, Rubinstein P, et al. Outcomes after transplantation of cord blood or bone marrow from unrelated donors in adults with leukemia. *N Engl J Med.* 2004;351(22):2265-2275.
36. Rocha V, Labopin M, Sanz G, et al. Transplants of umbilical-cord blood or bone marrow from unrelated donors in adults with acute leukemia. *N Engl J Med.* 2004;351(22):2276-2285.
37. Takahashi S, Iseki T, Ooi J, et al. Single-institute comparative analysis of unrelated bone marrow transplantation and cord blood transplantation for adult patients with hematologic malignancies. *Blood.* 2004;104(12):3813-3820.
38. Couban S, Simpson DR, Barnett MJ, et al. A randomized multicenter comparison of bone marrow and peripheral blood in recipients of matched sibling allogeneic transplants for myeloid malignancies. *Blood.* 2002;100(5):1525-1531.
39. Vigorito AC, Azevedo WM, Marques JF, et al. A randomised, prospective comparison of allogeneic bone marrow and peripheral blood progenitor cell transplantation in the treatment of haematological malignancies. *Bone Marrow Transplant.* 1998;22(12):1145-1151.
40. Nunez C, Nishimoto N, Gartland GL, et al. B cells are generated throughout life in humans. *J Immunol.* 1996;156(2):866-872.
41. Rossi DJ, Bryder D, Zahn JM, et al. Cell intrinsic alterations underlie hematopoietic stem cell aging. *Proc Natl Acad Sci U S A.* 2005;102(26):9194-9199.
42. Frasca D, Landin AM, Lechner SC, et al. Aging down-regulates the transcription factor E2A, activation-induced cytidine deaminase, and Ig class switch in human B cells. *J Immunol.* 2008;180(8):5283-5290.
43. Allman D, Miller JP. The aging of early B-cell precursors. *Immunol Rev.* 2005;205:18-29.
44. Stem Cell Trialists' Collaborative Group. Allogeneic peripheral blood stem-cell compared with bone marrow transplantation in the management of hematologic malignancies: an individual patient data meta-analysis of nine randomized trials. *J Clin Oncol.* 2005;23(22):5074-5087.
45. Shimabukuro-Vornhagen A, Hallek MJ, Storb RF, von Bergwelt-Baildon MS. The role of B cells in the pathogenesis of graft-versus-host disease. *Blood.* 2009;114(24):4919-4927.
46. Baker MB, Riley RL, Podack ER, Levy RB. Graft-versus-host-disease-associated lymphoid hypoplasia and B cell dysfunction is dependent upon donor T cell-mediated Fas-ligand function, but not perforin function. *Proc Natl Acad Sci U S A.* 1997;94(4):1366-1371.
47. Shono Y, Ueha S, Wang Y, et al. Bone marrow graft-versus-host disease: early destruction of hematopoietic niche after MHC-mismatched hematopoietic stem cell transplantation. *Blood.* 2010;115(26):5401-5411.
48. Miklos DB, Kim HT, Miller KH, et al. Antibody responses to H-Y minor histocompatibility antigens correlate with chronic graft-versus-host disease and disease remission. *Blood.* 2005;105(7):2973-2978.

Published OnlineFirst May 30, 2013; DOI: 10.1158/0008-5472.CAN-12-3814

Molecular and Cellular Pathobiology

Cancer Research

PML-RARα and Its Phosphorylation Regulate PML Oligomerization and HIPK2 Stability

Yutaka Shima, Yuki Honma, and Issay Kitabayashi

Abstract

The *PML* gene is frequently fused to the *retinoic acid receptor α* (*RARα*) gene in acute promyelocytic leukemia (APL), generating a characteristic *PML-RARα* oncogenic chimera. PML-RARα disrupts the discrete nuclear speckles termed nuclear bodies, which are formed in PML, suggesting that nuclear body disruption is involved in leukemogenesis. Nuclear body formation that relies upon PML oligomerization and its stabilization of the hypoxia-inducible protein kinase (HIPK)-2 is disrupted by expression of the PML-RARα chimera. Here, we report that disruption of nuclear bodies is also mediated by PML-RARα inhibition of PML oligomerization. PKA-mediated phosphorylation of PML-RARα blocked its ability to inhibit PML oligomerization and destabilize HIPK2. Our results establish that both PML oligomerization and HIPK2 stabilization at nuclear bodies are important for APL cell differentiation, offering insights into the basis for the most common prodifferentiation therapies of APL used clinically. *Cancer Res; 73(14); 4278–88. ©2013 AACR.*

Introduction

In human leukemia, specific chromosomal translocations result in the expression of fusion proteins promoting malignancy (1, 2). The *PML* gene is the target of the t(15;17) chromosome translocation that is observed in more than 90% of acute promyelocytic leukemia (APL) cases, in which fusion of the *PML* and retinoic acid receptor α (*RARα*) genes leads to the expression of the aberrant PML-RARα fusion protein (3–6). The PML protein normally forms discrete nuclear speckles in the nucleus called PML nuclear bodies; in these, PML recruits other proteins, including transcription factors such as p53 and acute myeloid leukemia 1 (7–9), transcription coactivators such as hypoxia-inducible protein kinase (HIPK)-2 and p300 (10, 11), SUMO (12), and DAXX (13, 14). Nuclear bodies have been implicated in the regulation of apoptosis, cellular senescence, and antiviral responses. It has been reported that PML stabilizes transcription coactivators, such as HIPK2 and p300, to assemble transcription factor/coactivator complexes within nuclear bodies (15). In contrast, nuclear bodies are disrupted in t(15;17) APL (12, 16–19); in the presence of the PML-RARα fusion protein, nuclear bodies appear as dispersed microspeckles in which HIPK2 is destabilized (15). All-*trans*-retinoic acid (ATRA) and As_2O_3, which are used clinically in APL, restore the normal appearance of nuclear bodies (12, 17, 19–21). In t (15;17) APL, it remains unclear that the disruption of nuclear bodies is related to leukemogenesis and that their restoration would lead to therapy. The molecular mechanism by which PML-RARα disrupts nuclear bodies has remained elusive, hampering progress in the understanding of leukemogenesis.

The present study reveals that PML-RARα blocks PML oligomerization and disrupts nuclear bodies, and that the effect is reversed upon cAMP/PKA-dependent phosphorylation of PML-RARα. In addition, pharmacologic activation of adenylyl cyclase by forskolin restores PML nuclear bodies and promotes ATRA-induced APL cell differentiation. Furthermore, nuclear body restoration induced HIPK2 stabilization. These results suggest that nuclear body formation is regulated by PML-RARα phosphorylation, and that the restoration of nuclear bodies is important for APL cell differentiation.

Materials and Methods

Cell culture, infection, and antibodies

293FT cells, which were purchased from Invitrogen, and U2OS cells were cultured in Dulbecco's Modified Eagle Medium (DMEM) supplemented with 10% fetal calf serum (FCS). Plat-E cells were obtained from Dr. T. Kitamura (University of Tokyo, Tokyo, Japan) and were cultured in DMEM supplemented with 10% FCS, 10 μg/mL blasticidin, and 1 μg/mL puromycin. NB4 cells and K562 cells were cultured in RPMI-1640 medium supplemented with 10% FCS. Anti-HIPK2 antibody was described previously (15). Other antibodies were purchased commercially: anti-HA (3F10, Roche and Y11, Santa Cruz), anti-FLAG (M2, Sigma), anti-Myc (9E10, Upstate), anti-tubulin (H235, Santa Cruz), anti-PML (16.1–104, Upstate; H238, Santa Cruz; 001, MBL), anti-SUMO (Zymed), anti-DAXX (Exbio), and anti-RARα (C20, Santa Cruz).

Authors' Affiliation: Division of Hematological Malignancy, National Cancer Center Research Institute, Chuo-ku, Tokyo, Japan

Note: Supplementary data for this article are available at Cancer Research Online (http://cancerres.aacrjournals.org/).

Corresponding Author: Issay Kitabayashi, Division of Hematological Malignancy, National Cancer Center Research Institute, 5-1-1 Tsukiji, Chuo-ku, Tokyo 104-0045, Japan. Phone: 81-3-3547-5274; Fax: 81-3-3542-0688; E-mail: ikitabay@ncc.go.jp

doi: 10.1158/0008-5472.CAN-12-3814

Published OnlineFirst May 30, 2013; DOI: 10.1158/0008-5472.CAN-12-3814

Plasmids

The PML, PML-RARα, and HIPK2 expression vectors were generated as described previously (15). PML and PML-RARα deletion mutants were generated by PCR using pLNCX-HA-PML IV or pLNCX-HA-PML-RARα as the template.

Immunoprecipitation and Western blotting

293FT cells were transfected with the desired vectors and lysed as described previously (15). Cell lysates and immunoprecipitates were fractionated on SDS-polyacrylamide gels and transferred onto nitrocellulose membranes (Amersham). The membranes were incubated with primary antibodies and horseradish peroxidase-conjugated secondary antibodies. The immune complexes were visualized by the enhanced chemiluminescence (ECL) or ECL-Plus technique (Amersham), and the images were analyzed by ImageGauge (FUJIFILM).

Immunofluorescence

U2OS cells were cultured in 4-well chamber slides and transfected as described previously (15). The cells were exposed to 50 μmol/L forskolin for 18 hours. After forskolin exposure, the cells were fixed and incubated with antibodies as described previously. PML-RARα–expressing mouse c-kit$^+$ cells were exposed to 50 μmol/L forskolin for 24 hours. NB4 cells were exposed to 50 μmol/L forskolin or 1 μmol/L ATRA for 24 or 72 hours. The cells were analyzed by the same techniques as U2OS cells. Images were captured on an Olympus microscope and analyzed by deconvolution.

Serial replating assay

pMSCV, pMSCV-HA-PML-RARα, pMSCV-HA-PML-RARα ΔE, pMSCV-HA-PML-RARα S704A, pMSCV-HA-PML-RARα S704D, and pMSCV-HA-HIPK2 were transfected into Plat-E cells using GeneJuice (Novagen), and supernatants containing retrovirus were collected 48 hours after transfection. C-kit$^+$ cells were selected from the femurs of C57BL/6 mice using CD117-specific MicroBeads (Miltenyi Biotech), transduced with retroviruses using RetroNectin (Takara), and plated in methylcellulose medium (M3434, StemCell Technologies). The cells were cultured and replated every 4 to 6 days in methylcellulose medium under G418 selection. The cells from the first round (empty vector and PML-RARα ΔE) or the third round (PML-RARα point mutants) of colonies were harvested and analyzed by using immunofluorescence as described above. With respect to HIPK2 stabilization, c-kit$^+$ cells were infected with retroviruses containing HA-HIPK2. The next day, the cells were infected with retroviruses containing wild-type or mutants of HA-PML-RARα. The cells were cultured in methylcellulose medium under G418 and puromycin selection. The cells of the third-round colonies were harvested and subjected to Western blot analysis.

RT-PCR

Reverse transcriptase PCR was conducted as described previously (15). HIPK2 mRNA expression was analyzed using the following primers: forward (5′-CCCCTCAAATACATTCGCCC-3′) and reverse (5′-TGGTGTCTTCAGTCTCCACAAAGG-3′). The glyceraldehyde-3-phosphate dehydrogenase primer set was described previously (15).

Flow cytometric analysis

Before incubation with anti-Mac1-FITC (M1/70, eBioscience), NB4 cells were preincubated with immunoglobulin G from rat serum (Sigma) to prevent nonspecific binding of the antibody. The stained cells were analyzed by JSAN (Bay Bioscience), and the results were analyzed using FLOWJO software.

Results

PML oligomerization is required for nuclear body formation

The coiled-coil domain of PML mediates homo-oligomerization and hetero-oligomerization (18, 22–24). We have previously shown that PML IV interacts with 2 transcription factors important for granulocytic differentiation, PU.1 and CAAT/enhancer-binding protein (C/EBPε; refs. 25, 26). Therefore, we used PML IV and a PML mutant lacking the coiled-coil domain (PML IV ΔCC; Fig. 1A). As expected, PML IV ΔCC could not form homo-oligomers (Supplementary Fig. S1A). Immunofluorescence was conducted to assess the localization of the PML IV ΔCC mutant. As shown previously (21, 27), wild-type PML IV localized to the nucleus and formed nuclear bodies of normal appearance; however, the PML IV ΔCC mutant was expressed uniformly throughout the nucleus and did not form nuclear bodies (Supplementary Fig. S1B). These results suggest that PML oligomerization is associated with nuclear body formation. HIPK2 is stabilized by PML in nuclear bodies and destabilized by PML-RARα (15). To test whether the PML mutant destabilized HIPK2, FLAG-tagged HIPK2 was cotransfected with HA-tagged PML IV or PML IV ΔCC. Results showed that PML IV stabilized HIPK2, which is consistent with previous observations (15); however, PML IV ΔCC destabilized HIPK2 (Fig. 1B). The destabilization was rescued by a proteasome inhibitor, MG132 (Fig. 1B). These results suggest that PML oligomerization is required for PML-mediated HIPK2 stabilization.

PML-RARα disrupts nuclear bodies; however, the molecular mechanism underlying this effect remains unclear. The defect in nuclear body formation by the oligomerization-deficient PML IV ΔCC mutant led to the hypothesis that PML-RARα may prevent PML oligomerization. To test this hypothesis, the effect of PML-RARα on nuclear body disruption was evaluated by immunofluorescence. Wild-type PML and PML-RARα are expressed in APL cells. The localization of PML is diffused in cells expressing PML-RARα (18). We transfected U2OS cells with expression vectors encoding FLAG-tagged PML IV and hemagglutinin (HA)-tagged PML IV or HA-tagged PML-RARα. PML nuclear bodies were detected using anti-FLAG antibody. As shown in Supplementary Fig. S2B, PML IV formed large, discrete, and distinct nuclear foci in the absence of PML-RARα (top) but small and disperse foci in the presence of PML-RARα (bottom). The oligomerization capacity of PML was subsequently assessed in the presence and absence of PML-RARα. As shown in Supplementary Fig. S2C, PML-RARα inhibited PML–PML interaction, suggesting

Published OnlineFirst May 30, 2013; DOI: 10.1158/0008-5472.CAN-12-3814

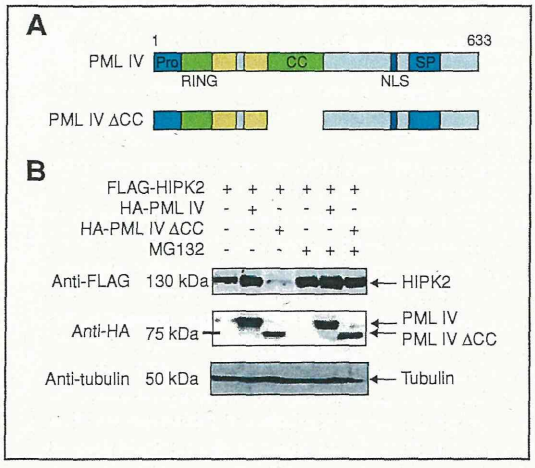

Figure 1. The coiled-coil domain of PML is required for HIPK2 stabilization. A, diagram of the PML deletion mutant. The proline-rich region (Pro), the ring-finger domain (RING), the coiled-coil domain (CC), the nuclear-import signal (NLS), and the serine-proline–rich region (SP) are indicated. B, PML IV ΔCC destabilizes HIPK2. 293FT cells were transfected with pLNCX-FLAG-HIPK2 and empty vector, pLPCX-HA-PML IV, or pLPCX-HA-ΔCC. The cells were treated with or without 10 μmol/L MG132 for 16 hours. The expression of HIPK2 (top), PML IV, or PML IV ΔCC (middle) and tubulin (bottom) was detected by immunoblotting using anti-FLAG, anti-HA and anti-tubulin antibodies, respectively.

that PML-RARα disrupts PML nuclear bodies by inhibiting PML oligomerization. The N-terminal or the coiled-coil domain of PML-RARα has been reported to be important for nuclear body disruption (28). PML 1–394, which is the PML moiety of PML-RARα and lacks the PML C-terminal, did not disrupt PML nuclear bodies (Supplementary Fig. S2D), suggesting that the RARα moiety of the fusion protein is also important for nuclear body disruption.

The ligand-binding domain of the RARα moiety of PML-RARα is essential for nuclear body disruption

Because the RARα moiety of PML-RARα is important for the disruption of PML nuclear bodies, PML-RARα deletion mutants were generated (Fig. 2A) to identify the region of RARα required for the effect. HA-tagged deletion mutants were cotransfected with FLAG-tagged PML IV. Immunofluorescence analysis indicated that PML-RARα 1–748 led to dispersed microspeckles, as did wild-type PML-RARα, but that deletion mutants lacking the ligand-binding domain, such as PML-RARα 1–567, 1–492, and 1–420, did not (Fig. 2B). These results suggest that the ligand-binding domain of RARα plays an important role in PML-RARα–mediated nuclear body disruption. The ΔE PML-RARα mutant, which lacks the ligand-binding domain (Fig. 2A), failed to disrupt nuclear bodies (Fig. 2B). The ΔC PML-RARα mutant, which lacks the DNA-binding domain, disrupted nuclear bodies (Fig. 2B). All of the PML-RARα deletion mutants were expressed at similar levels (Fig. 2C). We also tested the effect of the wild-type PML-RARα and the ΔE PML-RARα mutant on endogenous nuclear body formation in normal myeloid stem/progenitor cells. As the cells transduced with PML-RARα ΔE were not immortalized (Fig. 2D), we assayed for PML localization using the cells of first-round colonies with an anti-PML antibody specific for mouse Pml. Nuclear bodies were not disrupted in PML-RARα ΔE–infected cells (Fig. 2E). The localization of ΔE was different from that of wild-type PML-RARα. The ligand-binding domain of PML-RARα might be important for its dispersion. These results suggest that the ligand-binding domain of PML-RARα is indeed important for nuclear body disruption.

The effect of these PML-RARα mutations on HIPK2 stability was assessed. As shown in Fig. 2F, wild-type PML-RARα and PML-RARα 1–748, which disrupted nuclear bodies, destabilized HIPK2, whereas the other PML-RARα mutants, which did not disrupt nuclear bodies, did not destabilize HIPK2. To assess the effect of the same PML-RARα mutations on PML oligomerization, 293FT cells were cotransfected with Myc-tagged and FLAG-tagged PML IV together with HA-tagged PML-RARα mutants. As shown in Fig. 2G, immunoprecipitation and Western blotting indicated that wild-type PML-RARα and 1–748 inhibited the interaction between Myc-tagged and FLAG-tagged PML, whereas the other PML-RARα mutants did not. These results support the essential role of the ligand-binding domain of PML-RARα in the disruption of PML nuclear bodies.

The PKA phosphorylation site of PML-RARα is required for nuclear body disruption

Experiments were carried out to identify the sites responsible for PML nuclear body inhibition within the ligand-binding domain. As shown in Supplementary Fig. S3A, HA-tagged PML-RARα 1–708 or 1–661 was cotransfected with FLAG-tagged PML IV. PML-RARα 1–708 led to the formation of microspeckle PML nuclear bodies, whereas PML-RARα 1–661 did not (Supplementary Fig. S3B). These results indicate that the PML-RARα region spanning amino acids 662 to 708 is required for PML nuclear body inhibition. RARα and PML-RARα are phosphorylated by PKA (29, 30). Because serine 704, the PKA-dependent phosphorylation site of PML-RARα, is located within the region required for nuclear body disruption (Fig. 3A), mutants were generated in which serine 704 was substituted by alanine and aspartate to simulate dephosphorylated and phosphorylated serine, respectively. The effect of these mutants on PML nuclear body formation was assessed by the transfection of U2OS cells. Representative immunofluorescence data are shown in Fig. 3B (left), and the expression levels of PML and PML-RARα are shown in Fig. 3C. Quantification was done by counting the number of cells that formed large, discrete, and distinct PML nuclear foci in all transfected cells (Fig. 3D). Interestingly, wild-type PML-RARα and the alanine mutant (S704A) disrupted nuclear bodies, as shown by the presence of microspeckles, whereas the aspartate mutant (S704D) did not. Both mutants interacted with PML IV as strongly as did wild-type PML-RARα and the ΔE mutant (Supplementary Fig. S4), suggesting that the inability to disrupt nuclear bodies is not due to any deficiency in binding to PML. Forskolin was then used to activate adenylyl cyclase to

Published OnlineFirst May 30, 2013; DOI: 10.1158/0008-5472.CAN-12-3814

determine whether cAMP/PKA might restore nuclear bodies by phosphorylating the serine residue of PML-RARα. In the presence of forskolin, wild-type PML-RARα did not affect nuclear bodies (Fig. 3B and D); however, the S704A mutant, which lacks the serine residue phosphorylated by PKA, inhibited PML nuclear body formation even in the presence of forskolin.

We also tested the effect of wild-type and mutant PML-RARα in normal myeloid stem/progenitor cells. C-kit$^+$ mouse myeloid stem/progenitor cells were infected with a retrovirus encoding HA-tagged PML-RARα, HA-tagged S704A, or HA-tagged S704D and cultured in methylcellulose medium. The location of Pml in the immortalized cells was assessed using an anti-PML antibody specific for mouse Pml. Representative immunofluorescence data are shown in Fig. 4A, and quantification is shown in Fig. 4B. Nuclear body formation was maintained in S704D-expressing cells but was largely disrupted in wild-type PML-RARα- and S704A-expressing cells. The cells transduced with S704D were immortalized as well as those transduced with PML-RARα and S704A (Fig. 4C). Wild-type PML-RARα, S704A, and S704D were expressed at similar levels in the immortalized cells (Fig. 4D). Forskolin restored PML nuclear bodies in the wild-type PML-RARα–expressing cells but could hardly restore nuclear bodies in the S704A-expressing cells (Fig. 4E). These results suggest that the ability of PML-RARα to disrupt nuclear bodies is inhibited by cAMP/PKA-mediated phosphorylation of PML-RARα at serine 704.

Disruption of PML nuclear bodies by PML-RARα is strongly correlated with the destabilization of HIPK2 and the inhibition of PML oligomerization by PML-RARα

As shown in Fig. 1B and Supplementary Fig. S1B, PML IV ΔCC did not form nuclear bodies and destabilized HIPK2. Similarly, the PML-RARα deletion mutants that inhibited PML nuclear body formation also destabilized HIPK2 (Fig. 2F). These results suggest a correlation between nuclear body formation and HIPK2 stability. Therefore, the PML-RARα point mutants described above were assessed for their effect on HIPK2 stability. As shown in Fig. 5A, the level of HIPK2 decreased when HIPK2 was cotransfected with wild-type PML-RARα or S704A but not when HIPK2 was cotransfected with S704D. The effect of the point mutants on HIPK2 stability was also assessed in a stable system as shown in Fig. 4. Endogenous mouse HIPK2 could not be detected (data not shown). The expression of HA-tagged human HIPK2, introduced in mouse c-kit$^+$ cells, was detected only in S704D-expressing cells (Fig. 5B) of the third-round colonies. However, HIPK2 mRNA levels in cells expressing wild-type PML-RARα, S704A, or S704D were not appreciably different (Supplementary Fig. S5). These data support the hypothesis that HIPK2 destabilization is associated with PML nuclear body disruption. The point mutants were then assessed for their effect on PML oligomerization. S704A inhibited PML homo-oligomerization, as did wild-type PML-RARα, whereas S704D did not (Fig. 5C), implying that the protection of PML oligomerization from PML-RARα promotes PML nuclear body formation.

PKA-dependent phosphorylation of PML-RARα restores nuclear bodies and promotes ATRA-induced APL cell differentiation

As shown in Figs. 3–5, PKA-dependent phosphorylation of PML-RARα may be the switch that restores nuclear bodies. Cyclic AMP (cAMP) alone has no effect on nuclear body restoration, but cAMP and ATRA cooperatively restore nuclear bodies in NB4-R1 cells, which are ATRA-maturation–resistant cell lines (31). These data suggest that the cAMP/PKA pathway plays an important role in nuclear body formation. To determine whether the cAMP/PKA pathway actually regulates nuclear body formation in APL cells, APL-derived NB4 cells, which express endogenous PML-RARα, were exposed to forskolin alone. Nuclear bodies were detected using an anti-PML antibody; nuclear bodies were disrupted in NB4 cells, and became clear in the presence of forskolin (Supplementary Fig. S6A). Forskolin did not induce NB4 cell differentiation (Supplementary Fig. S6A). To characterize the forskolin-induced clear particles, the localization of SUMO and DAXX, which are recruited to nuclear bodies, was assessed using anti-SUMO and anti-DAXX antibodies. In the absence of forskolin or ATRA, the colocalization of SUMO and PML, or DAXX and PML, was very limited (Supplementary Fig. S6B). In contrast, ATRA restored nuclear bodies and recruited SUMO and DAXX to nuclear bodies. Forskolin changed the appearance of PML nuclear bodies from microspeckles to clear particles. In the clear particles, PML colocalized with SUMO and DAXX (Supplementary Fig. S6B). Thus, forskolin alone, like ATRA, restored nuclear bodies. ATRA induced PML-RARα degradation, whereas forskolin did not (Supplementary Fig. S6C). These data might reflect the smaller size of nuclear bodies in the presence of forskolin compared with that of ATRA. These data also suggest that PML-RARα phosphorylated by cAMP/PKA inhibits nuclear body disruption.

Because forskolin restored nuclear bodies in NB4 cells, the stability of endogenous HIPK2 was assessed in NB4 cells exposed to forskolin. As shown in Fig. 6A, forskolin increased HIPK2 protein levels but not HIPK2 mRNA levels. In contrast, forskolin did not increase HIPK2 protein levels in the non-APL K562 cells (Fig. 6B). HIPK2 protein levels increased in NB4 cells exposed to ATRA for 24 hours (Fig. 6C). Time-course analysis indicated that the increase in HIPK2 expression was correlated with nuclear body restoration (Fig. 6C and D). These results suggest that HIPK2 is stabilized in nuclear bodies restored upon cAMP/PKA-mediated phosphorylation of PML-RARα.

Finally, NB4 cells were exposed to forskolin or/and ATRA to determine whether nuclear body restoration may promote NB4 cell differentiation. As shown previously, forskolin was not sufficient to induce NB4 cell differentiation (Fig. 6E and F); however, forskolin enhanced ATRA-induced differentiation (Fig. 6E and F). The combination of ATRA and forskolin resulted in the differentiation of NB4 cells into segmented granulocytes (Fig. 6F) and increased the expression of the differentiation marker Mac-1 (Fig. 6G) more efficiently than either drug alone. Other studies have also shown the efficacy of cAMP against APL (32–35). These results and reports suggest that cAMP/PKA promotes ATRA-induced APL cell differentiation by restoring nuclear bodies.

Published OnlineFirst May 30, 2013; DOI: 10.1158/0008-5472.CAN-12-3814

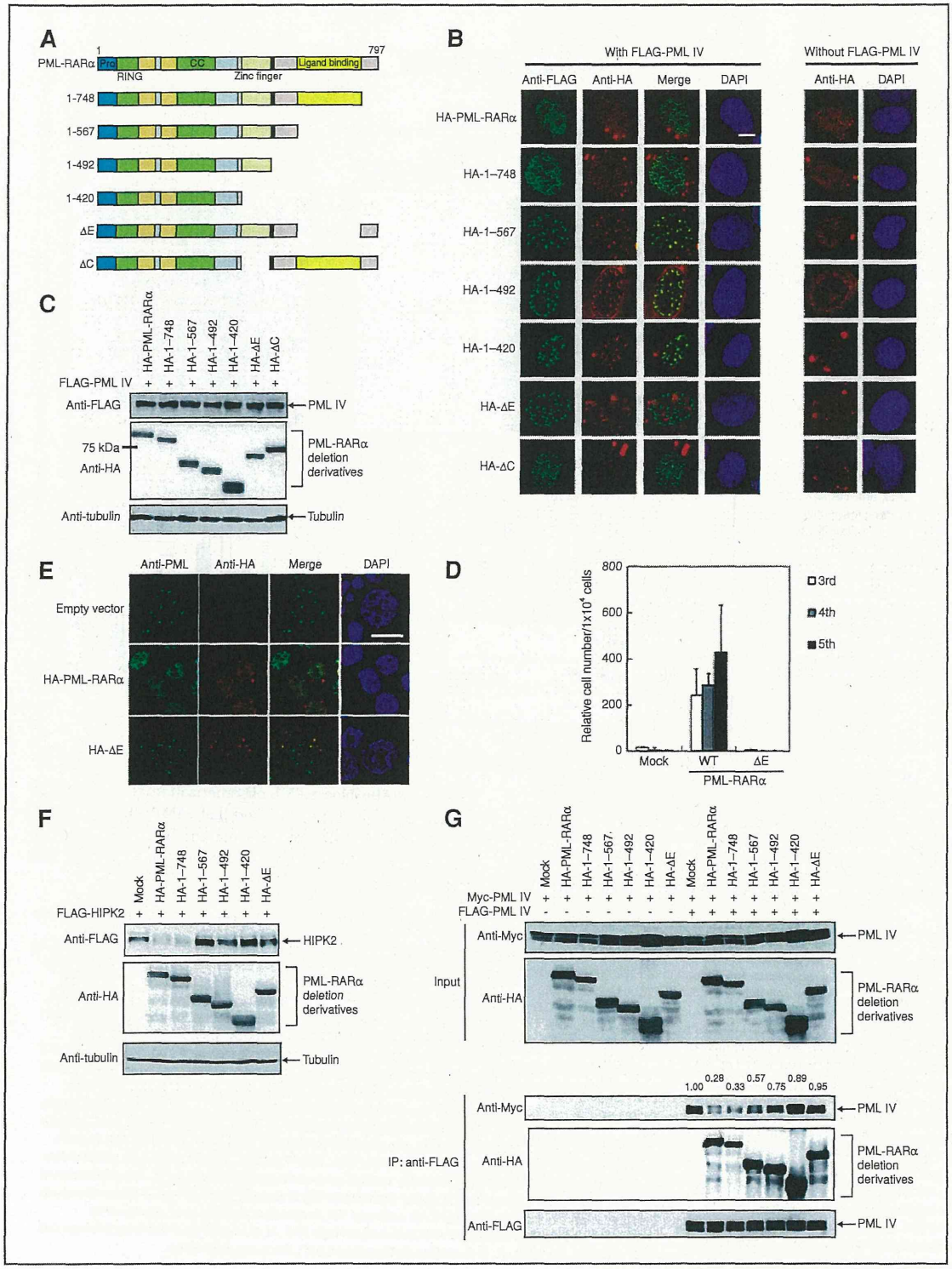

Published OnlineFirst May 30, 2013; DOI: 10.1158/0008-5472.CAN-12-3814

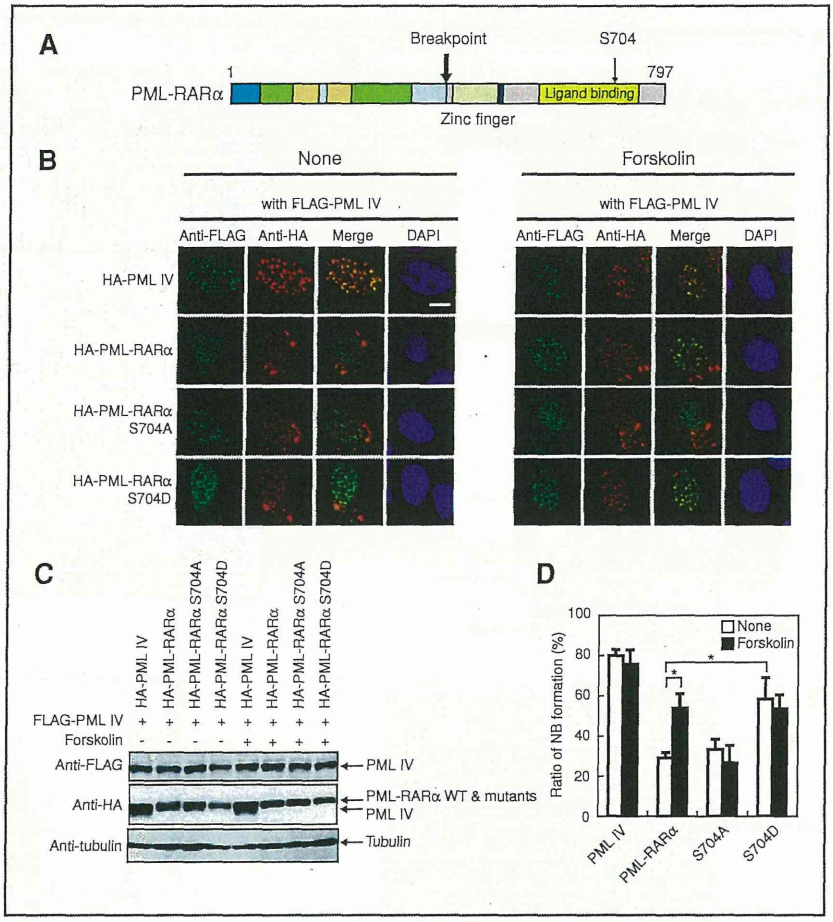

Figure 3. The PKA-dependent phosphorylation site of PML-RARα regulates PML nuclear body formation. A, diagram of the location of the PKA-dependent phosphorylation site of PML-RARα. B, phosphorylation of serine 704 is important for the restoration of PML nuclear bodies. FLAG-tagged PML IV and HA-tagged PML-RARα point mutants were coexpressed in U2OS cells. Cells were exposed to 50 μmol/L forskolin. PML nuclear bodies were analyzed using an anti-FLAG antibody. The white bar represents 10 μm. C, expression of PML-RARα wild-type and point mutants. The expression of PML IV (top), PML, PML-RARα wild-type or point mutants (middle), and tubulin (bottom) in U2OS cells was detected by immunoblot analysis with anti-FLAG, anti-HA, and anti-tubulin antibodies, respectively. D, quantification of nuclear body formation. The number of cells with PML nuclear bodies was counted. Values represent the mean ± SEM of 4 independent experiments. *, $P < 0.01$ compared with the PML-RARα value without forskolin. DAPI, 4′, 6-diamidino-2-phenylindole; NB, nuclear body.

Discussion

In more than 90% of APL cases, the PML-RARα fusion protein is generated by the t(15;17) chromosomal translocation. PML-RARα disrupts PML nuclear bodies by a mechanism that was not understood in detail. The present study reveals that PML-RARα blocks PML oligomerization, resulting in the disruption of nuclear bodies, and that cAMP/PKA phosphorylation of PML-RARα restores nuclear bodies. Our results suggest that nuclear body restoration enhances APL cell differentiation.

Figure 2. The ligand-binding domain of PML-RARα is essential for nuclear body disruption. A, diagram of PML-RARα deletion mutants. B, the ligand-binding domain of PML-RARα is required for the disruption of PML nuclear bodies. U2OS cells were transfected with pLNCX-FLAG-PML IV and pLNCX-HA-PML-RARα deletion constructs or only with pLNCX-HA-PML-RARα deletion constructs as described. PML nuclear bodies were analyzed using anti-FLAG antibody. The white bar represents 10 μm. C, expression of PML-RARα deletion mutants. The expression of PML IV (top), PML-RARα deletion mutants (middle), and tubulin (bottom) in U2OS cells was detected by immunoblotting using anti-FLAG, anti-HA, and anti-tubulin antibodies, respectively. D, the cells expressing PML-RARα ΔE are not immortalized. C-kit$^+$ mouse bone marrow cells were infected with empty vector (mock), pMSCV-HA-PML-RARα wild-type, or ΔE and cultured in methylcellulose medium. The colony number from the third to the fifth round of colonies is indicated (top). Values represent mean ± SEM from 3 independent experiments. E, PML-RARα ΔE does not inhibit nuclear body formation. C-kit$^+$ mouse bone marrow cells were infected with empty vector, pMSCV-HA-PML-RARα wild-type, or ΔE, and plated in methylcellulose medium. Endogenous murine PML nuclear bodies of the cells at first round of colonies were analyzed using mouse Pml-specific antibody (16.1~104). The white bar represents 10 μm. E, effect of PML-RARα deletion mutants on HIPK2 stability. 293FT cells were transfected with pLNCX-FLAG-HIPK2 and either empty vector or pLNCX-HA-PML-RARα deletion constructs. The expression of HIPK2 (top), PML-RARα deletion mutants (middle), and tubulin (bottom) was detected by immunoblotting using anti-FLAG, anti-HA, and anti-tubulin antibodies, respectively. G, effect of PML-RARα deletion mutants on PML oligomerization. 293FT cells were transfected with pLNCX-Myc-PML IV and either pLNCX-HA-PML-RARα deletion constructs or pLNCX-FLAG-PML IV (empty vectors were used as negative controls). The expression of Myc-tagged PML IV and HA-tagged PML-RARα deletion mutants in the lysates of transfectants was detected by immunoblotting using anti-Myc and anti-HA antibodies, respectively (input). The lysates of transfectants were incubated with anti-FLAG antibody. The immunoprecipitates were analyzed by immunoblotting using anti-Myc, anti-HA, and anti-FLAG antibodies (IP). The values of IP/input intensity of Myc-PML IV were quantified with ImageGauge and normalized to the value of Myc-PML IV/empty vector/FLAG-PML IV. DAPI, 4′, 6-diamidino-2-phenylindole; IP, immunoprecipitation.